2. Strain partitioning due to salt – insights from interpretation of a 3D seismic data set in the NW German Basin

Abstract

We present results from interpretation of a 3D seismic data set, located within the NW German sedimentary basin, as part of the Southern Permian Basin. We focused on the development of faults, the timing of deformation, the amount of displacement during multiphase deformation, strain partitioning, and the interaction between salt movements and faulting. We recognised the central fault zone of the study area to be the Aller-lineament, an important NW-trending fault zone within the superimposed Central European Basin System.

From structural and sedimentological interpretations we derived the following evolution: (1) E-W extension during Permian rifting, (2) N-S extension within cover sediments, and E-W transtension affecting both basement and cover, contemporaneously during Late Triassic and Jurassic, (3) regional subsidence of the Lower Saxony Basin during Late Jurassic/Early Cretaceous, (4) N-S compression within cover sediments, and E-W transpression affecting both basement and cover, contemporaneously during Late Cretaceous/Early Tertiary inversion, (5) major subsidence and salt diapir rise during the Cenozoic.

We suggest that the heterogeneity in distribution and timing of deformation in the working area was controlled by pre-existing faults and variations in salt thickness, which led to stress perturbations and therefore local strain partitioning. We observed coupling and decoupling between pre- and post-Zechstein salt units: in decoupled areas deformation occurred only within post-salt units, whereas in coupled areas deformation occurred in both post-salt and pre-salt units, and is characterised by strike-slip faulting.

2.1. Introduction

Numerous seismic surveys carried out by the oil and gas industry provided insight into the complex structural style and sedimentary record of sedimentary basins, like the NW German Basin. Primarily, 2D reflection seismic lines and well data were used for interpretations of important subsurface structures and basin-wide deformational processes (e.g. Baldschuhn *et al.,* 1996; Brink *et al.,* 1992; von Hartmann, 2003; Kossow & Krawczyk, 2002; Maystrenko *et al.,* 2005). Rare 3D reflection seismic measurements were carried out on a much smaller scale (von Hartmann, 2003; Mohr *et al.,* 2005). 2D seismic cross-sections are subject to spatial artefacts: the reflection patterns are affected by marginal effects, the profiles do not necessarily run perpendicular to the strike direction of the structural elements, and section balancing and calculation of material loss is arguable when mobile salt structures are involved. Therefore, 3D seismics are important to clarify still unsolved aspects in the evolution of the NW German Basin: e.g. the relationship among fault systems, the relationship between faulting and sedimentation, the kinematic regime during several deformational phases, the development and timing of inversion structures, as well as the coupling or decoupling between pre- and post-salt units, and the role of salt diapirism and the interaction between faulting and salt movements.

Many of these aspects are also essential for other sedimentary basins. The NW German Basin with its complex development is a good study area in which to gain insight into these aspects. Therefore, we have investigated the structural and sedimentological aspects of the study area with

a 3D seismic data set, to investigate the underlying processes behind the structures observed, and to compare them with the evolution of other neighbouring basins. The location of our working area within a key zone (Aller-lineament) of the Southern Permian Basin makes this study important to gain insights into the complex deformation history of this basin, and to understand more about the interaction between faulting and salt movements within sedimentary basins in general.

2.2. Tectonic setting

The NW German Basin is part of the European Southern Permian Basin (SPB), a specious epicontinental/intracontinental sedimentary basin developed on Variscan and Caledonian deformed crust. The NW-SE orientated SPB extends from the North Sea to Poland and varies in width between 300 and 600 km between Scandinavia and the Variscan Deformation Front (Fig. 2.1). It initiated in the Late Carboniferous to Permian, but subsequent multiphase deformation and salt migration over several hundred Ma affected not only the thick sedimentary cover, but also the older basement rocks, and divided the large basin in several sub-basins: Sole Pit Basin, Broad Fourteens Basin, Central Netherlands Basin, West Netherlands Basin, Central Graben, Horn Graben, NE German Basin, Polish Basin, as well as the Lower Saxony Basin, Pompeckj Block and Glückstadt Graben as part of the NW German Basin.

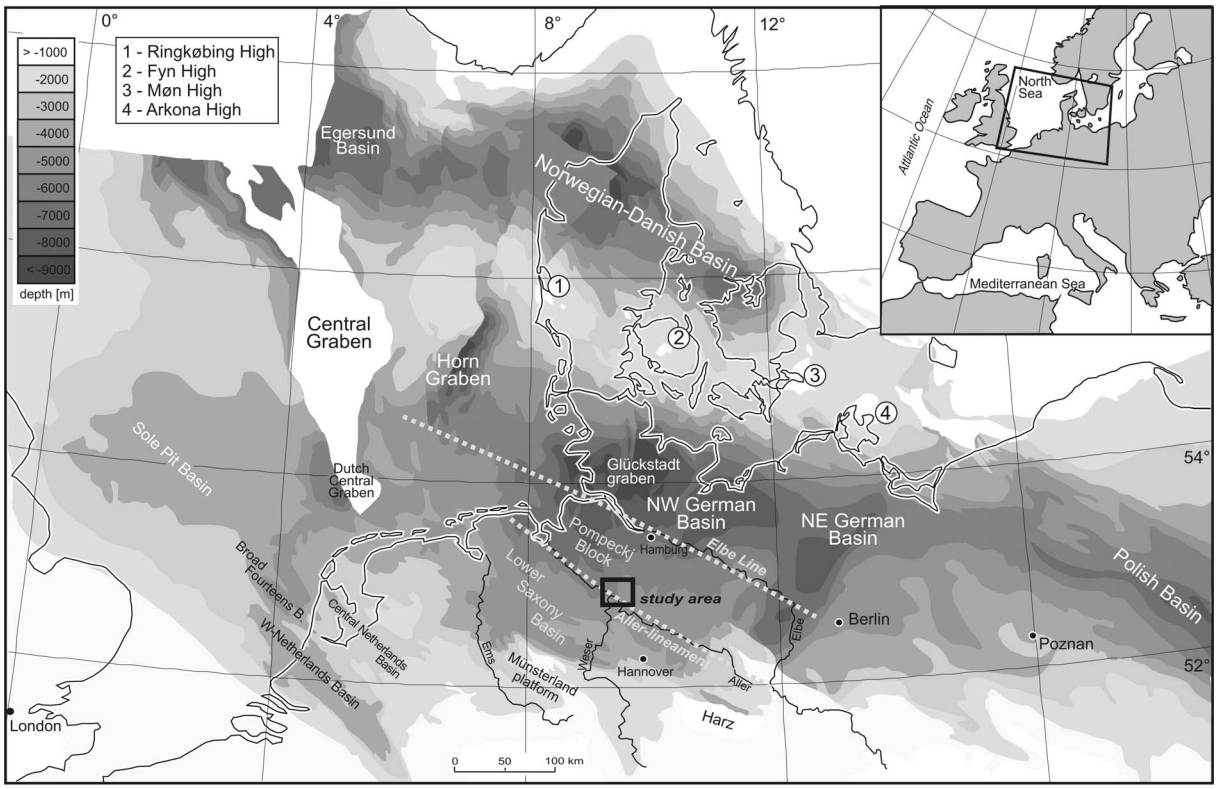

Figure 2.1: Depth map of the Southern Permian Basin and location of the study area. The NW-striking Aller-lineament forms the border between the Lower Saxony Basin in the south and the Pompeckj Block in the north, which represent two sub-areas of the larger NW German Basin. Modified after Kossow (2001) and the NW European Gas Atlas (Lockhorst 1998).

The general evolution of the Southern Permian Basin and its sub-basins is documented by e.g. Betz *et al.,* 1987; Glennie, 1998; Meissner & Bortfeld, 1990; Ziegler, 1990; Blundell *et al.,* 1992 and

references therein; Brink *et al.,* 1992; Pharaoh, 1999 and references therein; Krawczyk *et al.,* 1999 and 2002; Scheck-Wenderoth & Lamarche, 2005 and references therein.

In Central Europe, rifting and associated volcanism in the post-Variscan phase occurred in a dextral transtensional stress regime (e.g. Arthaud & Matte, 1977; Betz *et al.,* 1987; Ziegler, 1990) and produced mainly N-S orientated normal faults and NW-trending dextral strike-slip faults during the Late Carboniferous and Permian (e.g. Kockel, 2002; Gast, 1991 and 1988; Ziegler, 1990; Betz *et al.,* 1987). After the Middle Triassic, regional E-W extension opened NNE-SSW-trending grabens (e.g. Glückstadt Graben, Rheinsberg, Gifhorn, Hamburg and Jade-Westholstein Troughs (Scheck & Bayer, 1999; Maystrenko *et al.,* 2005)). Graben systems like the Permian Lower Saxony rift system (Gast, 1988 and 1991; Ziegler, 1990) and associated basins extend northwards via the Glückstadt Graben, the Horn Graben, and the Skagerrak Graben into the Oslo Graben (Gast, 1988 and 1991; Ziegler, 1990). Subsequently, the Southern Permian Basin thermally subsided coevally with deposition of Rotliegend clastics, followed by deposition of several kilometres of sediments from the Zechstein until the Quaternary (e.g. Baldschuhn *et al.,* 1996). During the Mesozoic and Cenozoic the area was affected by different processes such as salt movement, regional and differential subsidence, Triassic/Jurassic extension, as well as Late Cretaceous/Tertiary compressional phases and thereby associated basin-wide inversion processes (e.g. Schwab *et al.,* 1982; Betz *et al.,* 1987; Baldschuhn *et al.,* 1991; Brink *et al.,* 1992; Kossow *et al.,* 2000; Kockel, 2003; de Jager, 2003; Scheck-Wenderoth & Lamarche, 2005).

Within the NW German Basin, sub-areas developed during the Mesozoic. Our working area is located at the transition of two of them: the Lower Saxony Basin (LSB) located in the south, and the Pompeckj Block (PB) located in the north (Fig. 2.1). Only a few studies have been carried out investigating the evolution of these sub-areas more closely, especially the LSB, mainly based on 2D seismic interpretations (Baldschuhn *et al.,* 1985; Betz *et al.,* 1987; Brink *et al.,* 1992; Best, 1996; Mazur & Scheck-Wenderoth, 2005) and 1D well data (Gast, 1988; Hoffmann *et al.,* 2005), but only rarely on 3D seismic data (von Hartmann, 2003; Tanner *et al.,* subm.). The deformation within the LSB and the PB is very heterogeneous, and 1D or 2D investigations very often cannot resolve complex 3D structures. Especially the orientation of structures, and the timing of extension and inversion differ spatially, and the processes behind are not clearly understood. There are no significant vertical offsets within the basement of the LSB, the crustal configuration is largely unknown, and the role of salt and basement involvement is not completely answered.

The transition zone between the two sub-areas (LSB and PB) is the so-called Aller-lineament, a prominent NW-striking feature (Fig. 2.1). The lineament is a zone separating areas (LSB, PB) of different sedimentation (Best, 1996; Betz *et al.*, 1987; Hoffmann *et al.,* 2001; Kockel, 2003; Frisch & Kockel, 2003; Scheck-Wenderoth & Lamarche, 2005), characterised by a high occurrence of Zechstein salt structures (Baldschuhn *et al.,* 1996), and both vertical and horizontal movements (Stackebrandt & Franzke, 1989; Betz *et al.*, 1987). It has been described as a deep-seated Palaeozoic fault zone, which underwent polyphase reactivation during the Mesozoic and partly Cenozoic (e.g. Gast, 1988; Hoffmann *et al.,* 1998; Frisch & Kockel, 2003). Despite several investigations, the deformation style and the precise localisation of the Aller-lineament, as well as the correlation between basement structures and Mesozoic structures is not well determined.

Although Permian rifting (expressed by N-S oriented grabens) continued during the Triassic north of the Aller-lineament, the area south of the Aller-lineament experienced nearly no deformation during that time. The separation between the LSB and the PB started in the Late Jurassic, when the PB became uplifted and the regional Jurassic/Cretaceous unconformity developed. Contemporaneously, the LSB suffered differential subsidence due to divergent dextral movements along NW-SE trending fault systems, during which reactivation of Permo-

Carboniferous fault systems occurred (e.g. Aller-lineament) (Betz *et al.,* 1987). Inversion took place during the Late Cretaceous and was expressed predominantly as transpressive movement; but it was not synchronous in all parts of the LSB (Betz *et al.,* 1987). Especially the fault systems along the northern and southern margin of the LSB became reactivated, and the sedimentary fill was thrusted over the adjacent stable PB in the north and the Münsterland platform in the south (Betz *et al.,* 1987).

Caused by this evolution, today, in the LSB NW-striking faults dominate, whereas the PB is marked by mainly N- to NNW-striking faults. Together with the Elbe line, the Aller-lineament belongs to the NW-trending Elbe Fault System, along which a change in orientation of salt structures is observable (e.g. Jaritz, 1987; Lokhorst, 1998; Scheck *et al.,* 2003; Scheck-Wenderoth & Lamarche, 2005). North of the Elbe Fault System salt structures strike N-S, parallel to Triassic/Jurassic initiated grabens like the Glückstadt Graben, the Horn Graben, and the Central Graben (e.g. Ziegler, 1990; Lokhorst, 1998; Kockel, 2002). South of the zone salt structures strike mainly NW-SE, parallel to Jurassic/Early Cretaceous basins like the Sole Pit, the Broad Fourteens, and the LSB (e.g. Betz *et al.*, 1987; Ziegler, 1990; Lockhorst, 1998).

2.3. Data base

A pre-stack, depth-migrated, 3D reflection seismic data set and well data were provided by RWE-Dea AG, Hamburg, for this study. For interpretation, the seismic volume (17 x 22 km x 7.5 km depth) was loaded together with drill-hole information allowing a seismostratigraphic calibration (software: GeoFrame, Schlumberger). The 11 wells are located in the central part of the investigated area. The seismic data volume was interpreted, and reflections as well as picked horizons were checked for consistency. Fault surface geometries were also determined in 3D.

The seismic volume images the structures of the study area from the Carboniferous to the Quaternary. Generally, exploration drilling aims to reach the Upper Rotliegend, because it is the most exploited hydrocarbon-reservoir in the NW German Basin. Only rarely do wells penetrate Lower Rotliegend or Carboniferous rocks, and therefore these strata cannot continuously correlated across the whole area. In places, salt impaired the seismic interpretation by reducing the reflection energy underneath large salt domes, and by deforming overlying sediment reflections due to velocity pull-up. However, the overall data quality is good and enables detailed structural insights.

2.4. 3D structures

2.4.1. General stratigraphy

From correlation of well data the stratigraphy with its average thickness is summarised in Figure 2.2. Selected depth and thickness maps are shown in Figure 2.3, including the location of three seismic cross-sections (shown in Figs. 2.4, 2.5, 2.6), and the locations of wells (Fig. 2.3 c). Numerous unconformities have been recognised: within the Rotliegend, Base Zechstein, within the Buntsandstein, within the Lower and Upper Cretaceous, Base Tertiary, as well as several unconformities within the Quaternary. The major unconformities are marked in the stratigraphic overview (Fig. 2.2), but only the most important Jurassic/Cretaceous one is marked in the cross-sections (Figs. 2.5, 2.6).

The Carboniferous and Permian successions are quite similar throughout the study area (Fig. 2.2). Also the sedimentation during the Triassic is comparable, but differences in thickness exist between the northern and southern part of the area. The Jurassic/Cretaceous unconformity

truncates strata down to the Middle Jurassic in the southern part, but even down to the Upper Triassic in the northern part (Fig. 2.2). This led to a thick Jurassic succession of on average 1000 m in the southern part, whereas in the northern part these strata are absent. The thickness of Lower Cretaceous sediments differs in a complimentary manner: the northern part contains c. 800 m thick sediments, but only 150 m thick sediments in the southern part (Fig. 2.2). Only slight differences in thickness occur in the Upper Cretaceous and the Tertiary, where the sedimentary thickness increases gently towards the north.

Rheologically-weak rocks like salt can act as detachments. In the study area such detachment levels are recognised in the Zechstein and in the Middle Keuper (Fig. 2.2). The thickness of the mechanically weak Zechstein salt plays an important role in the evolution and structural style of the whole Southern Permian Basin, and is responsible for coupling or decoupling between pre- and post-Zechstein salt units. For that reason we distinguish between basement and cover in our working area. In this paper we define the pre-Zechstein salt units (Carboniferous, Rotliegend, and Zechstein anhydrite) as basement, but the post-Zechstein salt units (Mesozoic and Cenozoic rocks) as cover. The Top A2 horizon is a strong reflector representing an anhydrite of the lowermost Zechstein (Fig. 2.2), and marks the base of the Zechstein salt. It is the deepest regionally correlative seismic horizon.

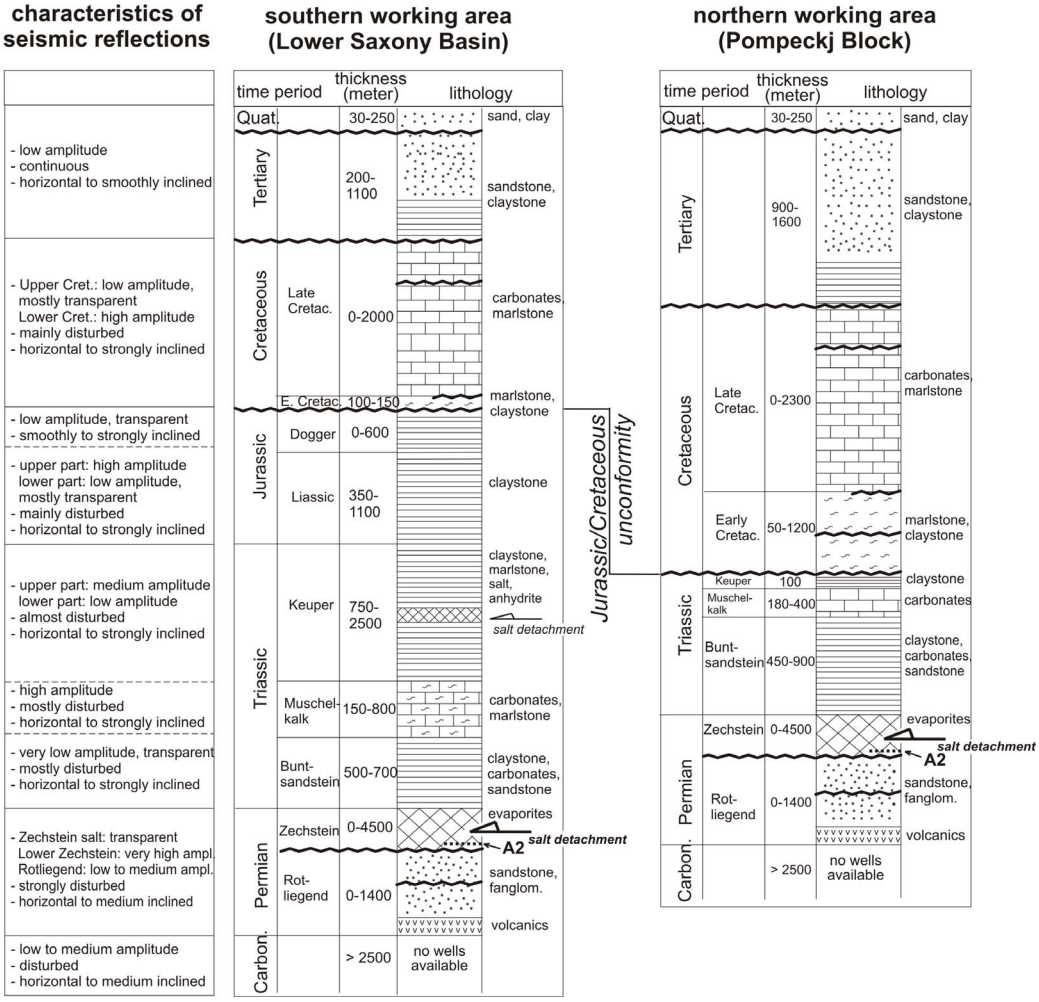

Figure 2.2: Generalised stratigraphy of the working area, separated for the Lower Saxony Basin (left) and the Pompeckj Block (right). The left column shows the general characteristics of seismic reflections. Lithology is normalised with the average thickness. Main unconformities are shown as sinuous lines.

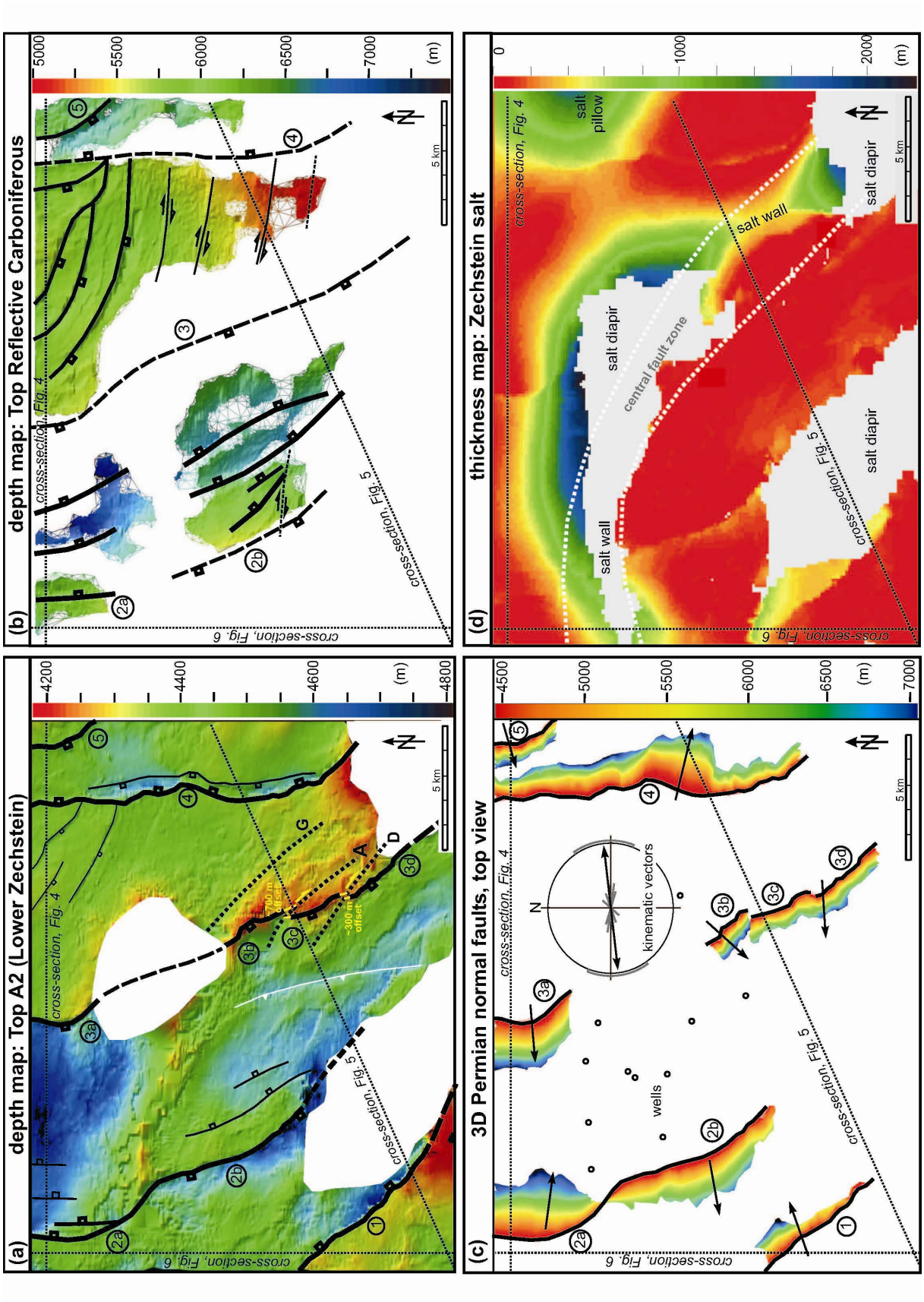
(a)
depth map: Top A2 (Lower Zechstein)
4200
4400
4600
4800
(m)
cross-section, Fig. 4
cross-section, Fig. 5
cross-section, Fig. 6
5 km
N
1
2a
2b
3a
3b
3c
3d
4
5
A
D
G
~700 m offset
~300 m offset
(b)
depth map: Top Reflective Carboniferous
5000
5500
6000
6500
7000
(m)
cross-section, Fig. 4
cross-section, Fig. 5
cross-section, Fig. 6
5 km
N
1
2a
2b
3
4
5
(c)
3D Permian normal faults, top view
4500
5000
5500
6000
6500
7000
(m)
cross-section, Fig. 4
cross-section, Fig. 5
cross-section, Fig. 6
5 km
N
wells
kinematic vectors
1
2a
2b
3a
3b
3c
3d
4
5
(d)
thickness map: Zechstein salt
0
1000
2000
(m)
cross-section, Fig. 4
cross-section, Fig. 5
cross-section, Fig. 6
5 km
N
salt pillow
salt wall
salt diapir
central fault zone
salt wall
salt diapir
salt diapir

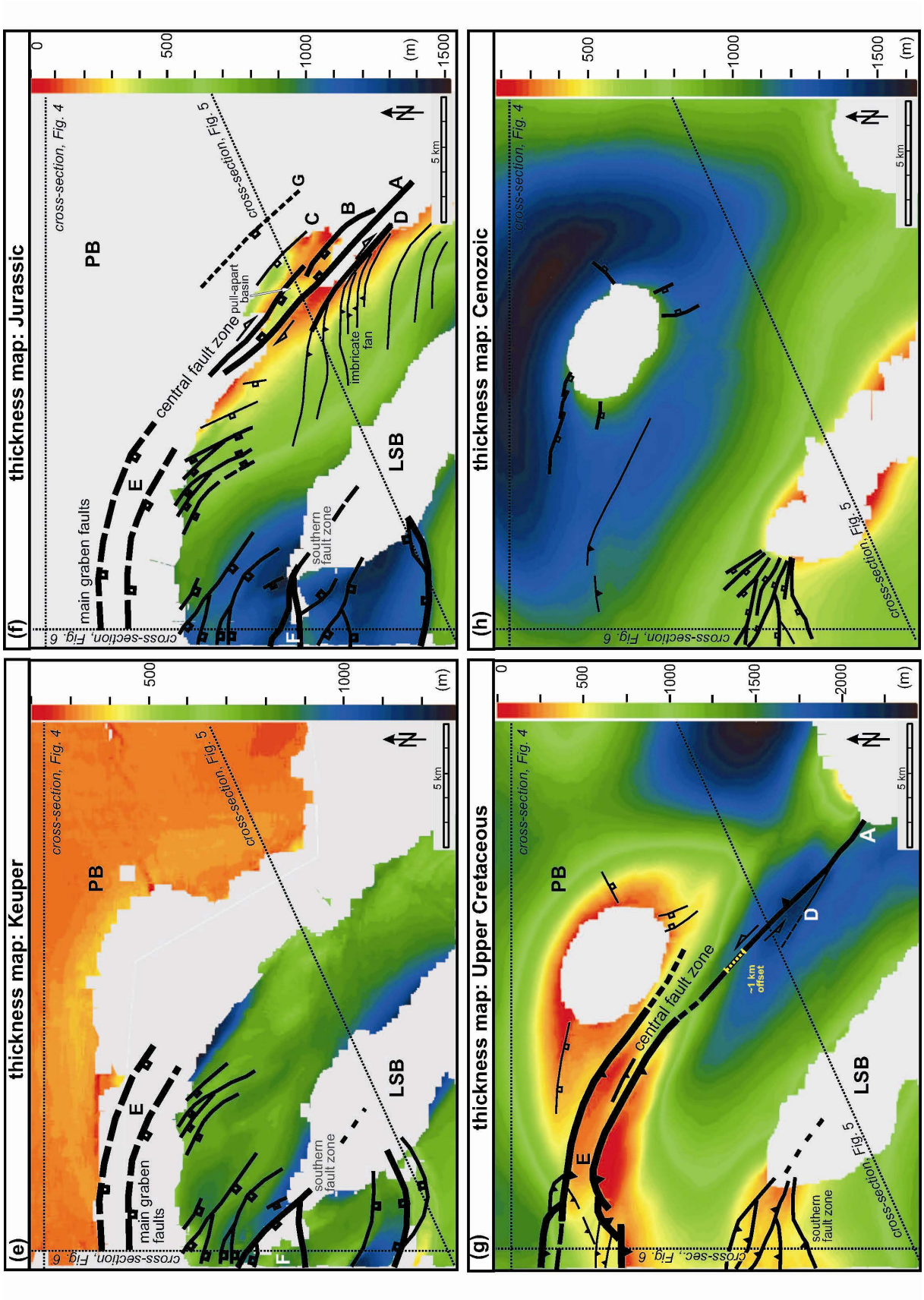
(e) thickness map: Keuper
(f) thickness map: Jurassic
(g) thickness map: Upper Cretaceous
(h) thickness map: Cenozoic
PB
LSB
main graben faults
central fault zone
southern fault zone
pull-apart basin
imbricate fan
cross-section, Fig. 4
cross-section, Fig. 5
cross-section, Fig. 6
~1 km offset
5 km
(m)

Figure 2.3 (previous pages): Depth maps and thickness maps of selected horizons with structural interpretation. Compare structures observed on these depth and thickness maps with those in the cross-sections (Figs. 4, 5, 6). (a) Top A2 (Lower Zechstein) depth map. Dotted lines indicate the traces at depth of faults A, D, and G. (b) Top Reflective Carboniferous depth map, (c) 3D interpretation of Permian normal faults, top view, coloured by depth. The strong convolution of faults 3b, 3c, and 3d is caused by Mesozoic strike-slip faulting. Arrows indicate kinematic movement direction determined from fault morphology analysis. Insert diagram shows all kinematic vectors, thick vector is the mean, bars on the circumference of the circle indicate the range of data. (d) Zechstein salt thickness map. The area between the dotted lines represents the region, which is effected by movements along the central fault zone. (e) Keuper thickness map, (f) Jurassic thickness map, (g) Upper Cretaceous thickness map, (h) Cenozoic thickness map. Uniform grey regions are uninterpreted areas, due to lower seismic resolution caused by salt (Fig. 3a, b, d, e, f, g, h), by strong faulting (Fig. 3b, e, f), or by the absence of strata (Fig. 3b, f). The central fault zone is interpreted as the boundary between the Lower Saxony Basin (LSB) and the Pompeckj Block (PB). Circled numbers and letters mark selected faults, which are also shown in the cross-sections.

2.4.2. Carboniferous/Permian deformation

Two depth maps (Top A2 horizon, Fig. 2.3 a, Top Reflective Carboniferous horizon Fig. 2.3 b), and one cross-section (Fig. 2.4) illustrate the Carboniferous/Permian deformation. Correlation with well data identified a strong reflector directly underneath the Zechstein salt as the Top A2 horizon between 4 and 5 km depth (Figs. 2.3 a, 2.4), traceable over the whole area. Below the Rotliegend formations, the next identifiable feature is a series of strong and continuous reflections. Since well information did not reach these depths we interpret these reflections to possibly represent Carboniferous Westfalian coal layers. These "reflective Carboniferous horizons" are c. 1500 m below the Top A2 horizon (Figs. 2.3 a, b, 2.4). The well-known stage of initiation of the North German Basin in the Permian is well documented in this study area.

The oldest identifiable structures are nearly E-W trending faults in the eastern part of the study area (Fig. 2.3 b); the faults are vertical, showing no vertical displacement, but a small horizontal displacement of a few hundred metres. Therefore, we interpret these faults as strike-slip faults having right-lateral offsets. We estimate that fault activation has occurred in the Late Carboniferous and/or Early Permian.

We recognised normal faults in depth maps (Fig. 2.3 a, b) and on cross-sections (Fig. 2.4) forming a system of grabens and halfgrabens, which affected Carboniferous to Permian rocks. Normal faults show orientations from NW-SE to N-S, and dip from 50° to 70°. Structural interpretation in a seismic section (Fig. 2.4) illustrates three Rotliegend horizons R1, R2 and R3 within the graben in the NW of the study area, and shows the synsedimentary tectonic evolution of this graben. The deepest horizon R1 in approximately 6 km depth is postulated as Base Rotliegend. At the western graben flank, faulting started with normal faults which formed a half graben. The thickness of the Rotliegend sediments (R1 - R2) varies between 350 and 600 m, reaching the highest thickness in the western and central parts of the structure. In Late Rotliegend, graben subsidence changed to the eastern flank, indicated by the thickness change of the Upper Rotliegend sandstones (R3 - Top A2), and the development of an angular unconformity above the R3 horizon. The thickness of these sediments varies between 140 and 520 m, with the highest value in the eastern part of the structure.

Synsedimentary normal faulting continued during the Lower Zechstein and produced a vertical displacement of 200 to 300 m at the Top A2 horizon. The amount of extension of the graben was calculated along the Base Rotliegend horizon with 2700 m (24.5 %), and along the Top A2 horizon with 300 m (2.7 %). Activity along these normal faults during the Triassic was not observed.

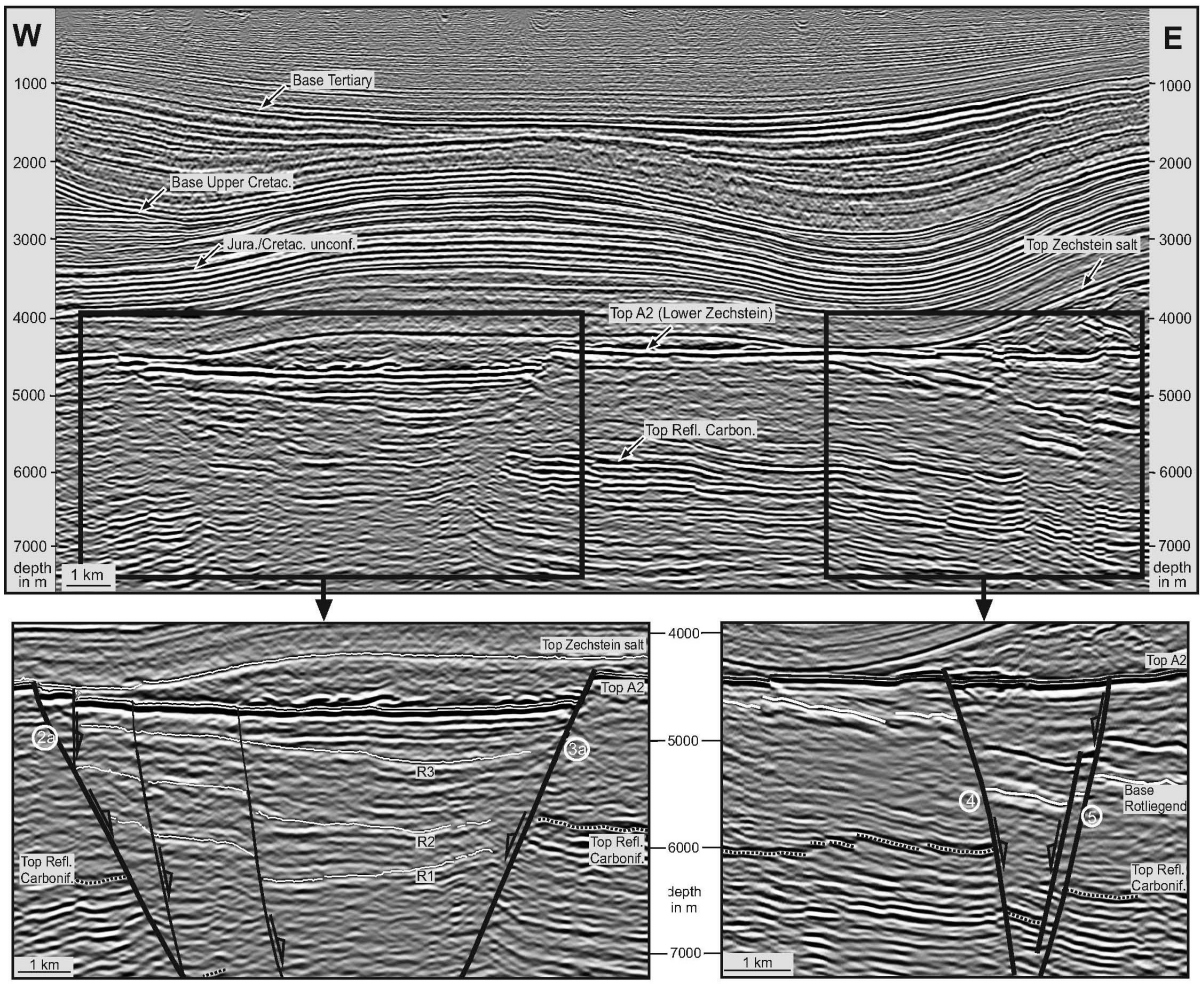

Figure 2.4: E-W oriented reflection seismic cross-section, shown as uninterpreted section (top) and with interpretations (bottom). Numbered faults as those in Fig. 3. Reflectors R1-R3 refer to Rotliegend horizons documenting Permian extension.

The synsedimentary tectonic evolution can also be observed within a smaller graben in the eastern part of the study area (Figs. 2.3 a, b, 2.4). Graben faults show a vertical displacement of 300 to 1100 m at the Base Rotliegend. Displacement at the Top A2 horizon reaches a maximum of 200 m. The amount of extension of the graben is calculated along the Base Rotliegend horizon with 250 m (14.3 %), whereas the extension along the Top A2 horizon is too small to have been measured. We assume that normal faulting probably started in the Early Permian and continued until the Late Permian.

NNW-striking normal faults have been identified in the north-eastern part of the area (Fig. 2.3 b). Because of their offsets in Carboniferous layers, we interpret them to have been initiated during Carboniferous or Early Permian. Very subtle offsets in the Top A2 horizon (Fig. 2.3 a) indicate either a continuous activity of these faults also during the Early Zechstein, or a higher compaction of Permian sediments within the hanging wall. The white coloured thrust fault at the Top A2 depth map is a Permian normal fault, which has been inverted during Late Cretaceous compression (see chapter 2.4.6).

Figure 2.3 c shows a map view of major Permian normal faults interpreted in 3D. The thick black lines represent the traces of faults on the Top A2 horizon. Coloured depth lines elucidate the undulation of the fault surfaces. The strike of these Permian graben faults, however, varies by 45°

between different faults, as well as along-strike of individual faults (Fig. 2.3 a, c, faults 2, 3, 4). Hence, the fault surfaces are strongly convoluted along strike. The undulations of fault planes result in varying dip directions of individual fault segments (in particular fault 4, Fig. 2.3 c). Therefore, we suggest that the presently-observed faults probably formed from smaller faults (c. 3 to 4 km) with varying dip, which coalesced through breached relay structures (for terminology refer to e.g. Trudgill & Cartwright, 1994; Walsh *et al.,* 2002 and references therein).

Moreover, we suggest that the slight undulation of fault surfaces reflects the orientation of the movement vector, because movement parallel to the axis of curvature should require least energy. However, the strong convolution between faults 3b, c, d (Fig. 2.3 c) was caused by Mesozoic strike-slip faulting along the central fault zone (will be explained in chapters 2.4.4. and 2.4.6.). To determine the orientation of the movement vector here, we studied the morphology of the Permian faults. The analysis of the fault topography highlights areas of similar curvature and cylindricity. These areas, if linear, were assumed to be fault corrugations. Our analysis suggests E-W to ENE-WSW directed movements (Fig. 2.3 c). Typically, as well as following fault corrugations, fault displacement is near parallel to the fault dip (i.e. dip-slip). The range of slip direction is approx. 45°, similar to the variation in fault strike (Fig. 2.3 c).

2.4.3. Zechstein salt

Zechstein evaporites cover the Carboniferous/Rotliegend grabens. The top and base of the Zechstein salt has been interpreted, and a thickness map was compiled (Fig. 2.3 d), indicating thickness variations of up to 1600 m. The top of the Zechstein salt is a single-phase continuous reflection, bounding the more transparent salt. These zones are easily detectable in the seismic image due to their high-amplitude reflections, and their almost vertical internal diffractions (e.g. Fig. 2.4). Today, the thickness of the Zechstein salt is very variable (0 to 1600 m in mapped areas, up to 4500 m at salt diapirs) due to halokinesis. The study area is characterised by several salt structures: three diapirs, two salt walls, and one salt pillow (Fig. 2.3 d). Salt rise into diapirs resulted in depletion of the salt around the diapir, which typically lead to the formation of marginal rim synclines in the sediments above. Along the margins of the diapirs, salt movement affected Mesozoic and Cenozoic sediments by upward bending (e.g. Figs. 2.5, 2.6). Diapirism started in Keuper and Jurassic (chapter 2.4.4.), but the main phase of diapirism was during the Late Cretaceous (chapter 2.4.6.), and the Cenozoic (chapter 2.4.7.).

2.4.4. Late Triassic and Jurassic deformation

Two thickness maps of Keuper (Late Triassic) and Jurassic (Fig. 2.3 e, f), and two seismic cross-sections (Figs. 2.5, 2.6) illustrate the Late Triassic to Jurassic deformation. The Keuper thickness map illustrates a strongly reduced, but constant thickness (c. 350 m) in the northern part, whereas in the southern part the thickness is much higher and shows stronger variations (500 to 1200 m) (Fig. 2.5). This southern part is characterised by E-W to NW-SE trending normal faults, which accumulated a high amount of sediments in their hanging walls during the Keuper (Figs. 2.3 e, 2.6). In section view (Fig. 2.6) we recognised normal faults bounding grabens and halfgrabens. The most prominent normal fault detached along a Middle Keuper salt layer, and soled out into the Zechstein salt. We determine this fault as main graben fault (marked with a bold line and labelled as E in Figs. 2.3 e, f, 2.6). The main graben fault proceeds into several imbricate listric normal faults, building a roll-over anticline and tilted blocks (Fig. 2.6). Minor faults in the hanging wall of the main graben fault developed primarily during the Keuper and Liassic, but in the Dogger displacement occurred predominately along the main graben fault, which led to a wedge-shaped synsedimentary accumulation of 400 m Dogger sediments on top of the roll-over. Faulting might have continued also until the Malm, or possibly until the Lower Cretaceous, but

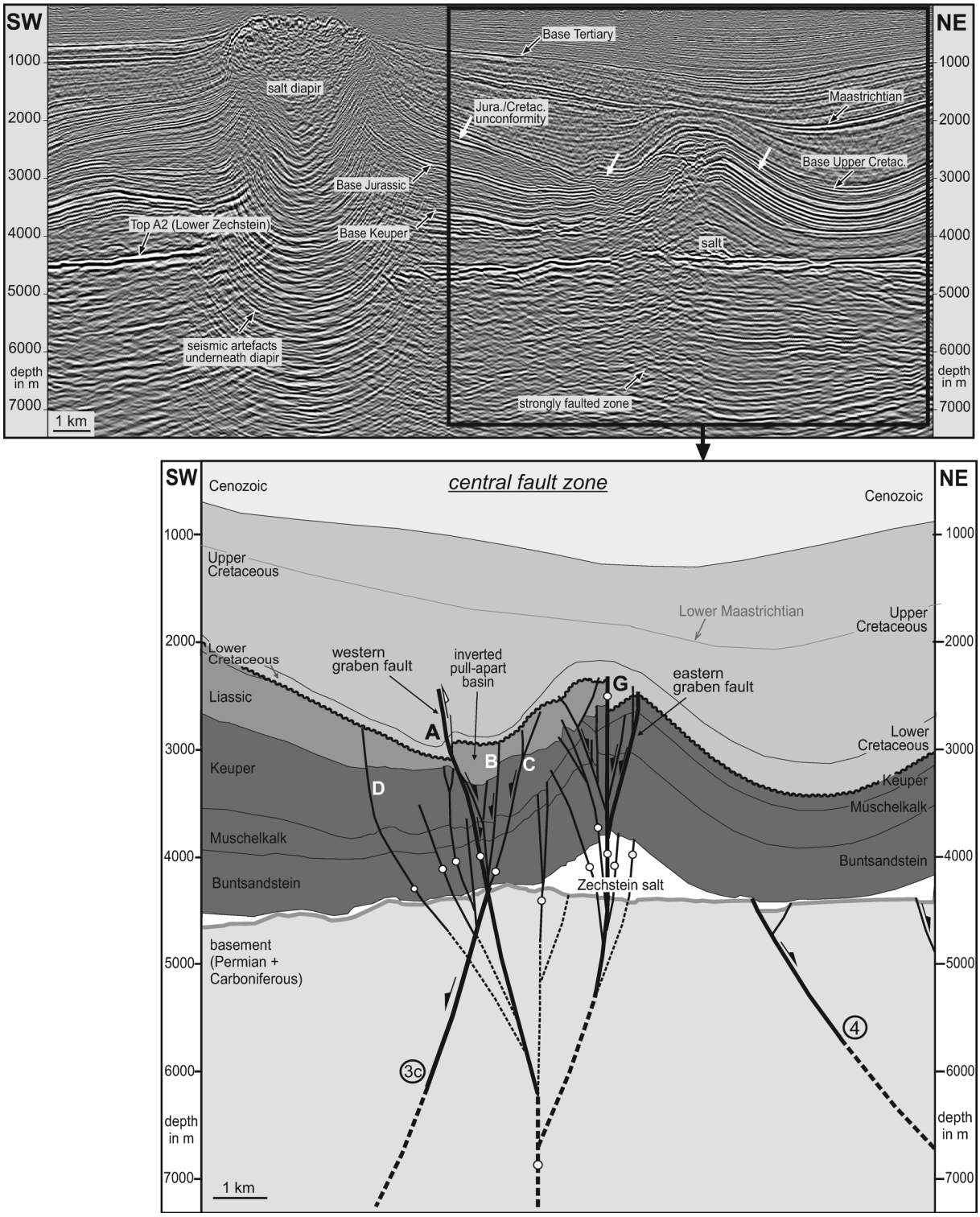

Figure 2.5: SW-NE oriented reflection seismic cross-section, shown as uninterpreted section (top) and with interpretations (bottom). Dotted faults are of uncertain location. White circles represent strike-slip faulting with undefined shear sense. Sinuous line marks the Jurassic/Cretaceous unconformity. The labelled faults A to D and G represent those in Fig. 2.3.

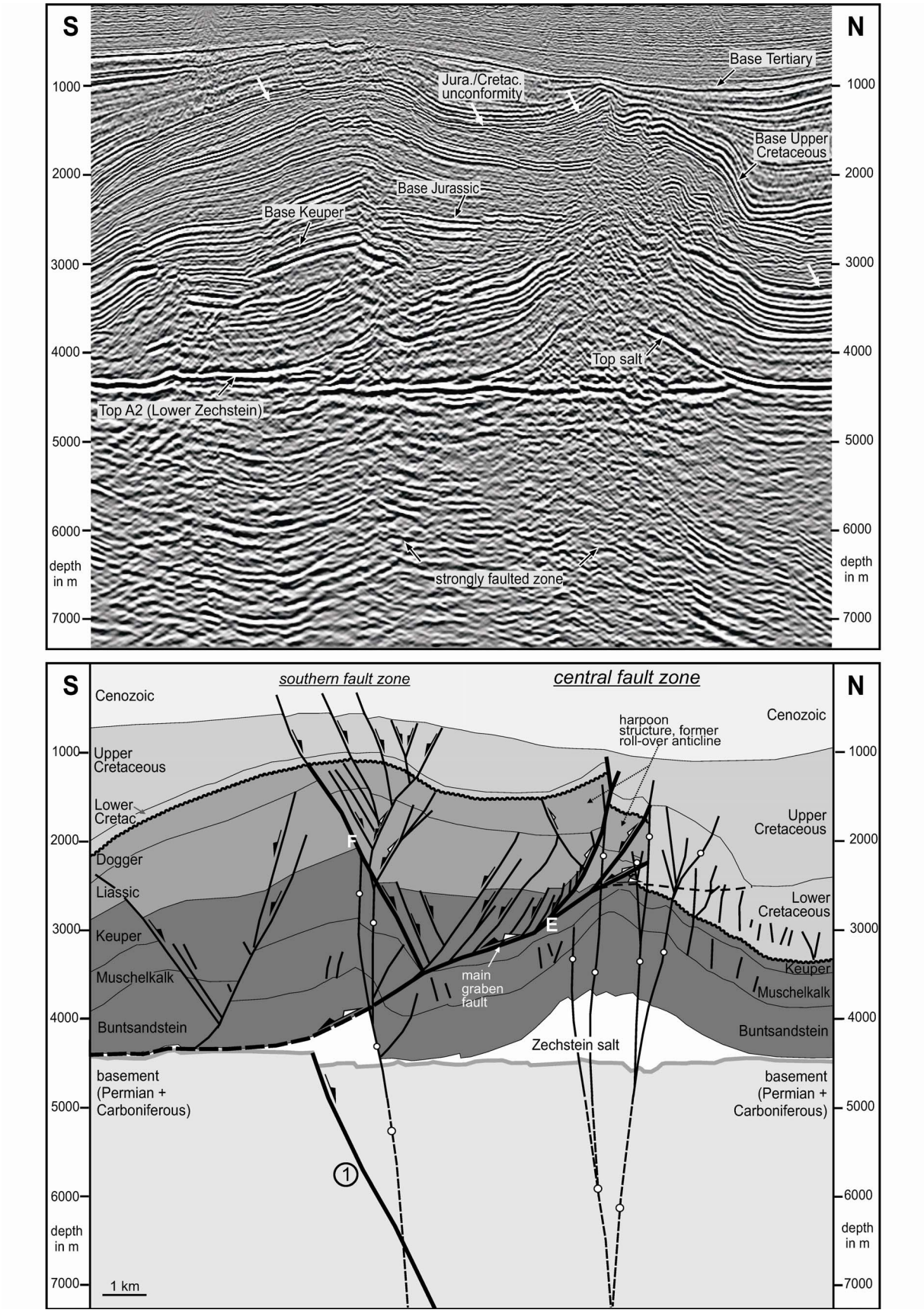

Figure 2.6: N-S oriented reflection seismic cross-section, shown as uninterpreted section (top) and with interpretations (bottom). Dotted faults are of uncertain location. White circles represent strike-slip faulting with undefined shear sense. Sinuous line marks the Jurassic/Cretaceous unconformity. The labelled faults E and F represent those in Fig. 2.3.

this cannot be proven because these sediments are eroded. Further to the south a normal fault (marked with a bold line and labelled as F in Fig. 2.6) developed antithetically to the main graben fault, synsedimentary during the Jurassic.

Steep faults characterise the eastern part of the study area. There is an increased thickness of Jurassic sediments (Fig. 2.5), which points to extension and graben development between fault A as western graben fault, and fault G as eastern graben fault. The Jurassic fault pattern (Fig. 2.3 f) illustrates NW-trending faults, bounding a basin between fault A and B (compare with Fig. 2.5). The basin is about 8 km long, and varies in width between 500 and 1000 m. During basin formation 300 to 400 m thick Liassic sediments were accumulated. The fault pattern could be interpreted as extensional system with relays, or as pull-apart basin. In the case of an extensional system, these normal faults could be newly formed during Jurassic and root into the Zechstein salt detachment, or they could be continuations of basement faults that have been reactivated. 3D seismic interpretations suggest a continuation of the Jurassic faults into the basement (Fig. 2.5). Comparison between basement faults and the Jurassic fault pattern demonstrates a difference in strike of structures of about 20° (Fig. 2.3 a, f). By following the Jurassic basin fault A into the depth (Fig. 2.3 a, f), its trace matches with a gap between the underlying Permian normal faults 3b and 3c. We interpret this gap to be caused by horizontal movement along steep faults. For these reasons we suggest that the Jurassic basin faults are not reactivated Permian normal faults, but they crosscut these faults and have been developed as transtensional faults forming a pull-apart basin, due to strike-slip faulting in the depth. However, in areas of fault intersections there could also be a reactivation of Permian normal faults by the Jurassic faults, but we exclude a reactivation over larger areas.

South of the pull-apart basin we detected steep faults, striking E-W, and dipping 50° to 90° mainly towards south (Fig. 2.3 f). The lower thickness of Jurassic sediments in their hanging wall indicates them as thrust faults. We interpret this fault pattern as contractional imbricate fan, which bends into fault D (Fig. 2.3 f). Both, the pull-apart basin and the imbricate fan can be explained by a superimposed transtensional regime during the Jurassic. However, because of the close location to a salt diapir in the south, it is likely that this thrust pattern is also influenced by local compression of the diapir.

The major fault systems which accumulated deformation during the Triassic and Jurassic (including faults A to G, Fig. 2.3 e, f) are aligned as NW-trending fault zone. Due to the importance of this zone (described as well in the next chapters) we determine this fault zone as the "central fault zone" of the working area.

2.4.5. Late Jurassic/Early Cretaceous deformation

The Jurassic/Cretaceous unconformity (Figs. 2.5, 2.6) truncates strata down to the Dogger in the S, but also down to the Keuper in the N. This unconformity shows an angular contact between Dogger and Lower Cretaceous strata in the south, but a conformable contact between Keuper and Lower Cretaceous strata in the N. Due to the different levels of erosion, the Jurassic strata have a thickness of up to 1500 m in the south, but in the north Jurassic strata are absent. The strong and parallel reflections of Lower Cretaceous sediments describe a high thickness of 400 to 800 m in the north, and a low thickness of only 100 m in the south (Figs. 2.5, 2.6). Within the Lower Cretaceous an angular unconformity can be recognised in the northernmost part of both lines. The reason for this unconformity is not detectable, due to the limited size of the study area.

Deformation in the Upper Jurassic/Lower Cretaceous was not observed along individual faults. However, across the NW-trending central fault zone the Mesozoic sedimentary style differs

strongly (see Figs. 2.3 e, f, 2.5, 2.6). The northern part of the study area is characterised by condensed Keuper sediments (constant 200 m thickness, Fig 2.3 e) and missing Jurassic sediments (Fig. 2.3 f), but an increased Lower Cretaceous sedimentation (50 to 1200 m thickness). The southern part contains 500 to 1200 m thick Keuper sediments and also Liassic and Dogger, but these Jurassic sediments thin out towards the NE (Fig. 2.3 f). Only 100 m of Lower Cretaceous are documented here.

2.4.6. Late Cretaceous deformation

The Upper Cretaceous thickness map (Fig. 2.3 g) and two seismic cross-sections (Figs. 2.5, 2.6) illustrate the Late Cretaceous deformation. The thickness map shows no differences between the northern and the southern part of the study area, but local differences because of salt diapir evolution. Areas of increased Upper Cretaceous thickness (more than 1250 m) represent salt rim synclines. Areas with reduced thickness are related to diapir growth, or to tectonic activity.

We recognised compressional faulting along the central fault zone, and along a fault zone further south (Figs. 2.3 g, 2.5, 2.6). Compressional deformation began after the Jurassic/Cretaceous erosional unconformity had developed, and led to inversion of the large graben structure (fault E in Fig. 2.6). Inversion was concentrated predominantly along the former main graben fault, which soled out into the Zechstein salt layer. However, the smaller-scale listric normal faults, which bound the tilted blocks, show almost no inversion. The reason for this preferred inversion along the main graben fault was probably due to a lower friction during gliding on the Middle Keuper salt detachment. The northernmost listric normal faults of the roll-over anticline were reactivated as several imbricate thrust faults (Fig. 2.6). The thereby produced harpoon structure incorporated a sedimentary Jurassic infill of several hundred metres (Fig. 2.6), covering an area of about 2 x 5 kilometres (Fig. 2.3 g). The vertical displacement along the imbricate thrust faults is several hundred metres, but bedding-parallel shortening along the former main graben fault is in the order of several kilometres. Correlation of tectonically controlled onlap structures with well data indicates that inversion occurred after the Coniacian and continued until the Maastrichtian, partly continuing until the Palaeocene.

In the eastern part of the working area we observed faulting along the central fault zone during the Late Cretaceous (Figs. 2.3 g, 2.5, 2.6). Reactivation is indicated by offset or bending of Upper Cretaceous reflectors, and by a reduced sedimentary thickness (Figs. 2.3 g, 2.5). We suggest that the Jurassic pull-apart basin (Fig. 2.3 f) has been uplifted, and changed into a pop-up structure during the Late Cretaceous, in which fault A was reactivated as thrust fault (Figs. 2.3 g, 2.5). Correlation with well data suggests that inversion along this fault occurred during the Santonian to Campanian. Vertical offsets vary between 100 to 200 m along strike. Due to abrupt changes in thickness of Upper Cretaceous sediments (Fig. 2.3 g), we interpret a sinistral horizontal offset along fault A of about 1 km. Dip-slip thrusting along this fault would have led to an apparent dextral offset of the isopachs, whereas the currently observable sinistral offset of 1 km is only possible with strike-slip or oblique-slip kinematics of more than 1 km. Further to the east, the area of fault G shows no evidence for faulting during Late Carboniferous (Fig. 2.5). However, the reduced thickness of Upper Cretaceous carbonates points to uplift in this area (Fig. 2.3 g). Onlap structures indicate uplift during Santonian to Maastrichtian of about 400 to 600 m along this zone. This uplift was probably caused by salt migration only, because changes in Zechstein salt thickness are in the same order (400 to 1000 m along this zone). Intense subsidence occurred during the Maastrichtian, which led to an accumulation of nearly 1000 m of sediments (Fig. 2.5).

The reduced thickness of Upper Cretaceous sediments in the area of the southern fault zone suggests uplift during that time (Figs. 2.3 g, 2.6). This uplift might have been caused by reactivation of the Jurassic graben fault F and its branch faults (Fig. 2.6).

In the area of the central fault zone underneath the two salt walls, we observed an upward bending of seismic reflectors, which we interpret as uplift of Upper Permian horizons. The Top A2 horizon is locally uplifted 100 to 300 m above the surrounding surface (Fig. 2.3 a). This uplift could be also a seismic artefact due to velocity pull-up underneath the salt walls (Fig. 2.3 d). However, the salt walls are not thick enough (average 500 m, Fig. 2.3 d) to cause such big artefacts; and numerous wells penetrating this zone (Fig. 2.3 c) provided evidence that the position of the Upper Permian horizons is correct. Furthermore, seismic reflectors underneath this zone have been strongly destructed vertically, which we interpret as vertical faults belonging to the central fault zone (Figs. 2.5, 2.6). Therefore, we interpret this uplift to be caused by horizontal movements along the central fault zone during Late Cretaceous inversion. Here, salt might have acted as free surface, and transpression than produced positive flower structures in the rocks underneath the salt.

2.4.7. Cenozoic deformation

Mesozoic faulting was followed by Cenozoic subsidence that is indicated by a widespread cover of Tertiary and Quaternary sediments. The Base Cenozoic erosional unconformity generally levelled the deformed pre-Cenozoic succession. Cenozoic strata are characterised by horizontal continuous reflectors diverging towards the N (from 500 m to 1200 m), which indicates higher subsidence further north (Fig. 2.3 h). Local thinning and thickening of strata occurs above or around salt diapirs and is primarily related to their Cenozoic rise or withdrawal.

The Cenozoic is characterised by a general tectonic quiescence. Salt rise during the Cenozoic probably initiated normal faulting around salt diapris (Fig. 2.3 h). Additionally, in the western part of the study area we observed faulting along the central fault zone (Fig. 2.3 h), which indicates minor compressional deformation during the Palaeocene (Lower Tertiary) as continuation of Upper Cretaceous inversion. Faulting occurred also along the southern fault zone. Here, normal faulting was initiated by salt rise of a nearby located diapir (Figs. 2.3 h, 2.6), and faults of the southern fault zone have been reactivated as dip-slip normal faults.

2.5. Discussion

2.5.1. Kinematics derived from structures

The basement of the whole study area is characterised by a system of mainly N- to NW-trending Permian graben faults, whereas post-Permian deformation is marked by mainly W- to NW-trending faults covering the Permian structures. Since the Jurassic, the sedimentation and the structural style led to a differentiation of the study area into a northern and a southern domain. Mesozoic deformation was concentrated primarily within the southern domain, whereas the northern domain was almost undisturbed (Fig. 2.3 e to h). For these reasons we interpret the central fault zone to be the Aller-lineament, which is the boundary between the Pompeckj Block to the north and the Lower Saxony Basin to the south. From fault pattern of the interpreted structures we derived the following kinematics (Fig. 2.7):

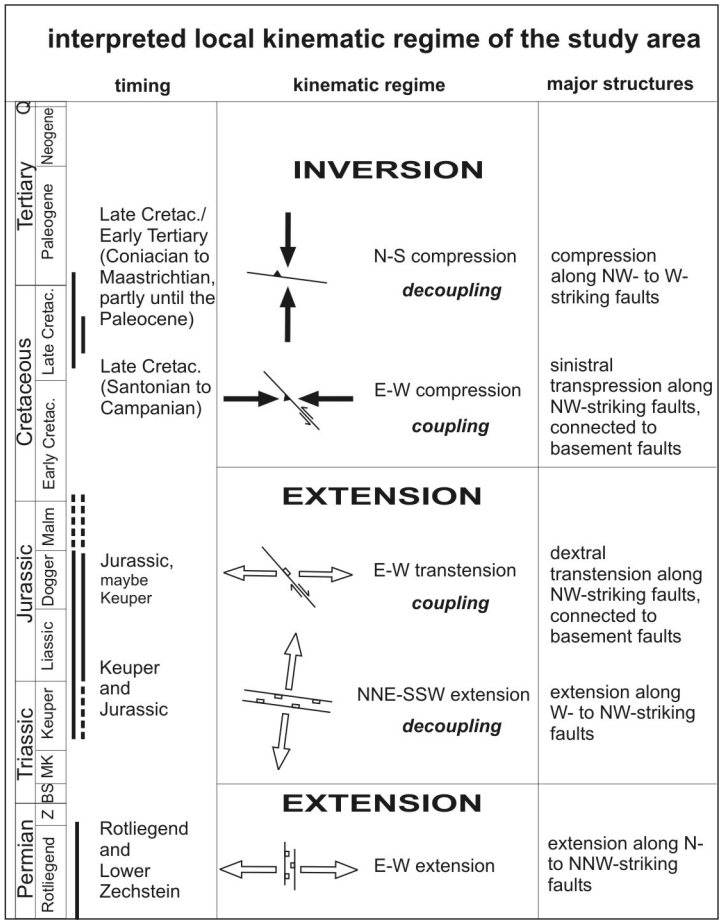

Figure 2.7: Summary of tectonic events for the study area, with major structures and derived kinematic regime. White arrows indicate horizontal extension direction; black arrows indicate horizontal compression direction. Abbreviations: Z - Zechstein, BS - Buntsandstein, MK - Muschelkalk, Q - Quaternary.

Carboniferous/Permian

Synsedimentary Permian extension produced a system of grabens and halfgrabens striking N to NW, which affected Carboniferous to Permian rocks. Rifting started probably in the Early Rotliegend and continued until the Early Zechstein. However, due to the limited depth of the wells the timing of onset of normal faulting can only be estimated. Orientation and kinematics of basement faults indicate an extensional kinematic regime during the Permian with nearly E-W horizontal extension direction (Figs. 2.3 c, 2.7). This coincides well with the overall suggested E-W extension and development of roughly N-S oriented grabens during the Latest Carboniferous to Permian (e.g. Ziegler, 1990; Betz *et al.,* 1987).

Late Triassic and Jurassic

Within the western part of the study area we interpret a NNE-SSW directed thin-skinned extension along NNW-trending normal faults during the Keuper (Upper Triassic) and Jurassic. Within the eastern part we propose a thick-skinned dextral transtension along NW-striking faults during the Jurassic, caused by horizontal E-W extension direction (Fig. 2.7). Whether transtensional movements within the basement continued also further to the west, and if they were active already during the Keuper, cannot be proven due to the occurrence of salt that hampers the resolution of the seismic data in this area. The timing of extension recognised in our working area is consistent with those of large N-S trending grabens further north, which initiated during the Triassic, like the Central Graben (Ziegler, 1990), the Horn Graben (Best *et al.,* 1983), and the Glückstadt Graben (Maystrenko *et al.,* 2005).

We calculated the horizontal displacement in the western part of the study area during thin-skinned Triassic/Jurassic extension, and determined an extension of c. 2 km. This minimum amount was calculated by (1) the sum of extension on each normal fault (along the Top Keuper strata) of the half graben between the two fault zones, and the graben in the southern part of the sections, (2) plus the required extension to accumulate the minimum 400 m thick Dogger sediments that form the roll-over anticline. However, the calculated amount is a minimum estimate, because of unknown thicknesses of Dogger and Malm sediments before erosion, and later inversion tectonics along the main graben fault.

We also calculated horizontal displacement during strike-slip faulting. By following the trace of faults A and D (Fig. 2.3 a, f, g) down to the Top A2 horizon, a horizontal offset of a Permian normal fault (3b, c, d in Fig. 2.3 a) is documented. Here, the normal fault is truncated, caused by horizontal movements along faults A and D. The apparent dextral offset of c. 700 m along fault A is the final result of Jurassic dextral and Late Cretaceous sinistral strike-slip faulting (this will be explained in chapter 2.5.1. *Late Cretaceous*). Both offsets (700 m along Top A2 depth map, and 1000 m in the Upper Cretaceous thickness map) suggest a minimum displacement of 1700 m along fault A during Jurassic dextral strike-slip faulting. The incremental and cumulative displacement along the prevailing fault A is not the absolute deformation along the whole strike-slip zone. Several smaller faults within this zone may have accumulated an additional amount of strain by horizontal offsets. Indeed, fault A accumulates a large amount of the total displacement during strike-slip faulting, but other parts of the fault zone may accumulate displacement in the same or higher order. However, because of salt occurrence within this zone, data quality is locally worse and complicates the calculation of superimposed displacements. Nevertheless, we assume that the total horizontal displacement at this part of the central fault zone amounts to only a few kilometres.

On a regional scale Ziegler *et al.* (2001) and Ziegler & Dezes (2006) described that during the Triassic and Jurassic a multi-directional rift system with associated wrench movements developed, which led to crustal separation in Western and Central Europe. During this deformation Permo-Carboniferous fracture systems were involved partly, and some areas (e.g. Central Graben, Horn Graben, Glückstadt Graben) underwent extensive crustal extension and crustal thinning (Ziegler *et al.,* 2001; Ziegler & Dezes, 2006). The area of the later LSB participated in that deformation only to a minor amount, expressed by the small N-S oriented Emsland Trough and Weser Depression. Therefore, this region appears to be the southernmost extent of intensive Triassic extension occurred further north, and the Aller-lineament might have acted as barrier zone that calmed any deformation further south.

Late Jurassic/Early Cretaceous

The primary sedimentary features are the thinning of Keuper sediments, the lack of Jurassic sediments, and an increase in Lower Cretaceous sedimentation north of the central fault zone with respect to the south. The high accumulation of Jurassic sediments within the southern part, and the high erosion within the northern part contemporaneously, could be explained by strong subsidence of the southern part with respect to the northern part, occurred during Early Cretaceous and/or Late Jurassic.

The contrasting pattern of sedimentation and erosion during the Late Jurassic/Early Cretaceous is recognised also throughout the NW German Basin, in which it is used to distinguish between the Pompeckj Block (PB) north of the Aller-lineament, and the Lower Saxony Basin (LSB) south of the Aller-lineament (e.g. Betz *et al.,* 1987; Best, 1996; Hoffmann *et al.,* 1998; Kockel, 2003; Frisch & Kockel, 2003, Scheck-Wenderoth & Lamarche, 2005). In the study area this

unconformity is documented in the north as a disconformity, whereas in the south it is a low-angle unconformity (Figs. 2.5, 2.6). Because we observed these typical sedimentation and erosion pattern in our study area, we interpret the area north of the central fault zone as Pomeckj Block, and the area south of the central fault zone as Lower Saxony Basin. The central fault zone itself is a key part of the Aller-lineament.

Comparing the LSB and PB in this study (Figs. 2.5, 2.6), the differences in sedimentation and erosion require either basement offsets, or strong salt movements to accumulate several kilometres of Jurassic sediments in the area of the LSB, and to contemporaneously erode strata down to Keuper in the PB. Extensive basin wide salt movements causing constant uplift of an area more than hundred km in diameter is rather unlikely, because salt would tend to rise inhomogenously, especially in areas with differences in sedimentary thickness, or strong faulting. Another possibility could be tectonically caused basement uplift. However, there is no evidence for significant basement offset along the Aller-lineament, neither in our study area, nor in other studies; but a tectonic uplift and later subsidence to exactly the same original level is very unlikely. However, another explanation could be a regional thermal uplift and later subsidence. Because Ziegler & Dezes (2006) suggested that during the Late Jurassic and earliest Cretaceous accelerated rifting activity occurred for example in the Central Graben of the North Sea rift, which was related to the development of shear systems at its southern termination, controlling the subsidence of trantensional basins like the Sole Pit, Broad Fourteens, West Netherlands, and Lower Saxony Basin. This transtensional concept for Jurassic/Cretaceous deformation for the LSB was also suggested by Mazur & Scheck-Wenderoth (2005) and Betz *et al.,* (1987). In the post-rift phase after the Late Jurassic/Early Cretaceous rifting, thermal subsidence of the North Sea Basin began, and affected also areas further south (Ziegler & Dezes, 2006).

Late Cretaceous

Within the western part of the working area we observed inversion along W- to NW-striking faults, which led to thin-skinned thrusting along Zechstein and Keuper salt detachments. To explain this fault pattern, we interpret a N-S compression direction. A minimum amount of 2 km inversion during N-S compression can be calculated by the displacement of the several imbricate thrust faults (Fig. 2.6). However, this amount is also a minimum estimate due to the minimum estimated amount of extension before inversion. In this western part inversion occurred from the Coniacian and continued until the Maastrichtian, partly continuing until the Palaeocene (Fig. 2.6).

Further to the east we identified faulting along NW-striking faults. Figure 2.3 g shows changes in thickness of Upper Cretaceous sediments on both sides of fault A, producing a bending of the isopachs of about 1000 m. Simple top-SW thrusting along fault A would led to an apparent dextral offset of the isopachs, whereas the currently observable sinistral offset of 1000 m is only possible with strike-slip or oblique-slip kinematics of more than 1000 m. Therefore, we suggest that along fault A occurred a minimum sinistral horizontal offset of 1 km during thick-skinned transpressional inversion tectonics, and we derive a horizontal compression direction of roughly E-W. Inversion took place during Santonian to Campanian, which is documented by onlap-structures of the Upper Cretaceous carbonates (Fig. 2.5).

At the Top A2 depth map we identified a N-S trending fault, which we interpret as a Permian normal fault that has been inverted during Late Cretaceous compression (white coloured thrust fault in Fig. 2.3 a). The timing of reactivation was determined to be Late Cretaceous because fault orientation fits to the proposed E-W compression during this time, the only compressional phase observed in the study area. However, an offset of Mesozoic horizons could not be identified, maybe due to decoupling and buffering of overlaying Zechstein salt during that time. This fault is

the only Permian normal fault that has been later inverted; all other large normal fault remained not reactivated. The reason for this preferred reactivation could be its gentle dip, which makes it easier to reactivate than the other large and steep normal faults. Additionally, apart from the reactivation of steep strike-slip faults, we assume that basement inversion in this area might have occurred only at a small-scale that affected mainly faults and fractures below the seismic resolution. That means, that the basement underwent shortening even though in a scale below the seismic resolution, but it might be significant for calculation of shortening in crustal-scale.

The timing of inversion observed in our working area is comparable with the general inversion of the LSB identified by other studies (e.g. Betz *et al.,* 1987; Kossow & Krawczyk, 2002; Mazur & Scheck-Wenderoth, 2005), but also with other basins along the southern margin of the SPB, like the Sole Pit, Broad Fourteens, and Netherlands Basins (de Jager, 2003 and references therein). There are minor differences in the timing of inversion between the several basins, which are mainly caused by the preferred reactivation of inherited structures depending on their orientation to the regional stress field (de Jager, 2003). Differences within the LSB might be related mainly to the selective nature of 2D seismic lines, in which differences between salt-related or fault-related unconformities are not easily resolvable.

On a regional scale, Late Cretaceous inversion of the LSB is caused by roughly NW-SE convergence between the European and African plates (e.g. Ziegler, 1982, 1990; Betz *et al.,* 1987). In our study area, heterogeneous fault patterns associated with Late Cretaceous inversion indicate that deformation varied temporally from the Coniacian to the Palaeocene along strike of the central fault zone. We identified coupling (involving basement and cover) associated with E-W transpression, and decoupling (involving only cover) associated with N-S compression. We assume that the contrasting local stress fields are caused by coupling/decoupling between basement and cover, which might have led to stress partitioning of the regional NW-SE convergence regime into a E-W component and a N-S component.

Vertical uplift during Late Cretaceous inversion is demonstrated by the difference in stratigraphic depth of the Jurassic/Cretaceous unconformity between the Lower Saxony Basin (LSB) and Pompeckj Block (PB). Since the amount of extension (during Keuper/Jurassic normal faulting), and the amount of compression (during Late Cretaceous inversion) are in the same order, the amount of vertical uplift is equivalent to the thickness of Keuper and Jurassic sediments accumulated within the LSB. We calculated an uplift of 1 to 2 km of the LSB with respect to the PB in our working area. This amount of vertical movement coincides with values of other locations: e.g. Van Wijhe (1987) proposed a 2 to 2.5 km uplift of the Broad Fourteens Basin, the hanging wall of the Harz Northern Fault was uplifted more than 4 km (Kockel, 2003), Kossow & Krawczyk calculated an upthrust of 3.5 km along the Gardelegen Fault within the NE German Basin, and the uplift of the Mid-Polish trough is estimated at 2 to 2.5 km (Dadlez *et al.,* 1997).

Cenozoic

The Cenozoic is characterised by subsidence and contemporaneous salt diapir rise with normal faulting. Only in the western part of the working area we observed tectonically induced faulting (Fig. 2.3 h), which we interpret as continued Late Cretaceous N-S compression along the central fault zone throughout the Palaeocene (Lower Tertiary).

Similar to our study area, other authors (Scheck-Wenderoth & Lamarche, 2005; Mazur & Scheck-Wenderoth, 2005; Maystrenko *et al.,* 2005) also described a general increase of subsidence towards the north, in the area of the Pompeckj Block. The continuation of Alpine collisional processes during the Palaeocene involved broad lithospheric folding and faulting, but led also to

an accelerated subsidence of the North Sea Basin throughout the Cenozoic (Ziegler, 1990; Ziegler & Dezes, 2006).

2.5.2. Deformation around the Aller-lineament

Deformation along the central fault zone, which we interpret to be a part of the Aller-lineament, indicates activity at least since the Keuper, but reactivation and inversion continued during the entire Mesozoic and partly to the Lower Tertiary. The subdivision of the NW German Basin into the Lower Saxony Basin (LSB) and the Pompeckj Block (PB) along the Aller-lineament has been recognised by a period of subsidence during Jurassic and Early Cretaceous, not only in this study area, but also in the whole LSB (e.g. Betz *et al.,* 1987; Kockel, 2003; Mazur & Scheck-Wenderoth, 2005).

In the study area, roughly NNE-SSW directed extension is inferred for the Keuper and Liassic, which led to the development of listric graben faults. The main graben fault is part of the Aller-lineament, and dips toward the south (Figs. 2.3 c, d, 2.6). The kinematic regime required for the fault patterns observed in the study area, has been recognised neither in the LSB nor in the PB on a larger scale. Instead, during this time, several N- to NNE-striking elongated grabens (e.g.: Central Graben, Horn Graben, Glückstadt Graben, Emsland Trough, Weser Depression) developed, indicating E-W extension. However, in the south-eastern prolongation of the Aller-lineament, south of the Flechtlinger High, Best (1996) recognised in several 2D seismic lines graben faults similar to those observed in our study area. He described listric normal faults dipping toward the SW, which developed during Late Triassic and Early Jurassic times. The main graben fault crops out at the surface and its lateral extension corresponds to the Aller-lineament (Best, 1996). Movement along this fault was accommodated primarily by a detachment on Zechstein salt, but subordinately also on an internal unit of Upper Buntsandstein salt (Best, 1996). The structures described by Best (1996) refer to a NE-SW-orientated horizontal extension direction during Keuper and Liassic (Early Jurassic). Due to the similarity in timing and orientation of structures in both study areas, we suggest the same deformational mechanism underlying the structures observed in this study. Because of the relative local occurrence, we propose that the extensional style at this time is typical for the area along the Aller-lineament.

Jurassic deformation produced a complex fault pattern of dip-slip and oblique-slip normal and thrust faults, as well as strike-slip faults, contemporaneously within the study area (Fig. 2.3 f). Heterogeneous fault patterns associated with Upper Cretaceous inversion indicate that deformation varied temporally from the Coniacian up to the Palaeocene over short distances, along a 24 km long part of the central fault zone (Fig. 2.3 g). Furthermore, comparing the different timing of Upper Cretaceous inversion of the study area with those of the LSB indicates that deformation of the study area varies in the same manner as in the whole LSB (e.g. Betz *et al.,* 1987; Baldschuhn *et al.,* 1991; Kockel, 2003). At the scale of the analysed data, the regional boundary conditions are obscured by local ones.

We suggest that the heterogeneity in distribution and timing of deformation along the Aller-lineament is not primarily caused by regional boundary conditions, such as the regional stress regime, but rather by local ones. One reason might be the existence and orientation of older faults, as they can act as weak zones and are therefore preferable for reactivations. Another important parameter is the variation of salt thickness through time, as it can produce detachment levels depending on the stage of salt movement. Furthermore, salt walls can also act as weak zones preferable for faulting. For these reasons we suggest that both pre-existing faults and diapirism led to stress perturbations and therefore local strain partitioning. Additionally, areas with higher salt thickness trigger a decoupling of the stress field between basement and cover.

Therefore, we explain the different stress regimes identified in our working area, with stress partitioning: During Late Cretaceous inversion, stress partitioning led to a differentiation of the regional NW-SE convergence regime into an E-W compressional component affecting primarily the basement, and a N-S compressional component affecting only the cover in our working area. The N-S extension that occurred during Triassic/Jurassic within the cover might have caused only subsequently as result of the development of accommodation space and subsequent salt rise, due to regional E-W extension and consequent transtension along the Aller-lineament. Therefore, we do not agree with Best (1996) that N-S extension initiated salt migration along the Aller-lineament. Instead, we suggest that transtensional faulting within the basement triggered salt migration, which finally initiated local N-S extension within the cover.

Furthermore, the Aller-lineament could have acted as stress concentrator which might have reduced the magnitude of Triassic/Jurassic E-W extension to continue towards the south. South of the Aller-lineament, the area of the LSB underwent only minor extension resulting in the formation of the Emsland Trough in the outer west and Weser Depression in the outer east (Betz *et al.,* 1987), but the central parts of the LSB subsided only moderately.

2.5.3. Interaction between faulting and salt movements

Salt migration started in Keuper and Jurassic, but the main phase of diapirism was during the Late Cretaceous and Cenozoic (Figs. 2.5, 2.6), which resulted in the three diapirs identified within the working area. The location of salt walls, connecting the diapirs, corresponds with zones of intense Mesozoic fault activity (Fig. 2.3 d). Uplift of Mesozoic sediments along the salt walls and the subsidence around their rims, indicates the formation of the salt walls during the Late Cretaceous, but it stopped before the Maastrichtian (Fig. 2.5). Conversely, Cenozoic subsidence led to a higher accumulation of sediments immediately above the uplifted area (Fig. 2.5), which was maybe caused by removal of salt due to the growth of surrounding diapirs (Fig. 2.3 h). In the investigated area, we observed that strike-slip tectonics along the central fault zone (during Jurassic and Late Cretaceous) involved the basement, and is therefore also associated with uplift of Upper Permian horizons. On the other hand, we recognised that during non-strike-slip tectonics (Triassic/Jurassic extension, Late Cretaceous thrusting) Zechstein salt and Middle Keuper salt acted as detachment levels in which fault systems sole out, but basement faults have not been involved during this deformation. Decoupling even led to different deformation styles in the same area, as it is shown in the western part of the central fault zone: thrusting of Mesozoic sediments (imbricate thrusts) occurred contemporaneously with oblique thrusting (positive flower structure) of Upper Permian sediments during the Late Cretaceous.

We assume that the present-day location of salt structures in the working area is not necessarily significant for assumptions of coupling or decoupling between cover and basement in former times, because it depends primarily on salt migration through time, and the deformation style. However, the timing of salt migration and faulting, and the present-day location of salt walls and fault zones, refer to an interaction between faulting and salt movement, and might be caused either by fault-induced salt migration, or by salt-induced faulting, or by a combination of both. Salt-induced faulting would produce only localised structures above the salt, but not underneath. Fault-induced salt migration would produce more elongated salt structures, directly located along the fault zones. In our working area we observed a combination of salt diapirs (development: Keuper to Cenozoic) and salt walls (development: only during Late Cretaceous). Mesozoic faulting localised not only above the salt, but also underneath the salt, involving the basement. Therefore, we assume that the fault- and salt-pattern observed in our study area have been caused by a combination of both, fault-induced salt migration, and salt-induced faulting. Salt migration and faulting initiated contemporaneously during (a) Keuper/Jurassic: transtensional faulting

within the basement triggered salt migration, which initiated local N-S extension within the cover, and (b) Late Cretaceous: salt wall development was strongly related with deformation along the central fault zone. Salt can move easily along tectonically weak zones; at the same time faulting is much easier along salt walls (e.g. Jackson & Vendeville, 1994; Stewart & Coward, 1995; Davison *et al.,* 1996; Rowan *et al.,* 1999).

This study supplements other regional studies in the NW German Basin (e.g. Brink, 1986, 1991; Scheck *et al.,* 2003; Mazur & Scheck-Wenderoth, 2005), which also suggest that the development of salt structures seems to be closely related to strike-slip or normal faulting. By analysing regional 3D structural models, Scheck *et al.* (2003) demonstrate that major changes in salt dynamics in the North German Basin are coupled with changes in the regional stress field. Tectonic activity initiated salt movement, which led to salt rise within fault zones. Periods of tectonic quiescence are characterised by a removal of salt out of fault zones. We assume that the development of the LSB and the PB was mainly controlled by tectonic activity along the Aller-lineament, but the preferred occurrence of salt structures in this area was responsible for stress perturbations and strain partitioning. The differences in the kinematic regime between the area of the Aller-lineament and other areas of the Central European Basin System might be mainly caused by the occurrence and distribution of salt structures, the evolution of salt structures through time, as well as the scale the data have been investigated.

2.5.4. Comparison with other basins of the Southern Permian Basin

The LSB has been developed along the southern margin of the Southern Permian Basin (SPB), together with other basins like the Sole Pit, Broad Fourteens, West Netherlands, and Central Netherlands Basin. They show a similar evolution in terms of sedimentation and timing of deformation, and developed within the same superimposed regional stress field; but differences exist in the distribution and thickness of the Zechstein salt (e.g. Lockhorst, 1998; Ziegler *et al.*, 2001; de Jager, 2003; Scheck-Wenderoth & Lamarche, 2005). However, the evolution of salt plays an important role, as it strongly controls the deformation style, and defines coupling or decoupling between pre- and post-salt units, and therefore the involvement of inherited structures during later deformation.

During Late Cretaceous inversion, the Polish Basin for example showed coupling in its south-eastern part, whereas the north-western part is marked by decoupling (Lamarche *et al.,* 2002). The NE German Basin, located west of the Polish Basin, is also characterised by decoupling between pre- and post-Zechstein salt units (Scheck & Bayer, 1999; Kossow *et al.*, 2000). Hansen *et al.* (2007) studied the northern part of the NE German Basin (western Baltic Sea) and demonstrated a high salt thickness (up to 7500 m inside diapirs) and thin-skinned tectonics during Mesozoic deformation. Further west of the LSB de Jager (2003) compared basins in the western part of the SPB and illustrated that basins without Zechstein salt (e.g. southern part of the Broad Fourteens Basin, West Netherlands Basin, Sole Pit Basin) are coupled and deformed mainly by strike-slip faulting, whereas basins that contain a high salt thickness (e.g. northern part of the Broad Fourteens Basin) are decoupled and not deformed by strike-slip faulting, but show an acceleration of halokinesis and different deformation styles above and below the salt. Late Cretaceous inversion affected those basins without Zechstein salt mainly by dextral strike-slip faulting along NW-striking reactivated basement structures (de Jager, 2003 and references therein). In contrast, the LSB contains a higher salt thickness and therefore shows only a minor internal deformation during inversion, and reactivation of basement structures occurred mainly along the northern and southern basin borders (Betz *et al.,* 1987). The differences in deformation style between the several sub-basins of the SPB might be mainly caused by the occurrence and

distribution of salt structures, defining coupling or decoupling between pre- and post-salt units, which subsequently trigger the reactivation of the different inherited structures.

2.6. Summary

(1) We determined the evolution of the study area, which includes E-W extension during Permian, N-S extension and E-W transtension during Late Triassic and Jurassic, regional subsidence of the Lower Saxony Basin during Late Jurassic/Early Cretaceous, E-W transpressional and N-S compressional inversion tectonics during Late Cretaceous/Early Tertiary, as well as subsidence and salt diapir rise.

(2) We interpret the central fault zone in the study area to be the Aller-lineament, the boundary between the Lower Saxony Basin (LSB) and Pompeckj Block (PB).

(3) We measured the horizontal displacement during extension and inversion within the sedimentary cover of the study area. The calculated minimum value of 2 km (during extension, and during inversion) underestimates actual deformation due to erosion of Jurassic sediments. The total horizontal displacement along the Aller-lineament, which involves both basement and cover, amounts to only a few km.

(4) The heterogeneity in distribution and timing of deformation in our study area is controlled by different reactivation of pre-existing faults depending on their orientation, and by salt distribution. These factors led to stress perturbations and therefore local strain partitioning: areas with higher salt thickness triggered a decoupling of the stress field between pre- and post-salt units. Therefore, we explain the different stress regimes between basement and cover, but also along strike of the Aller-lineament, with stress partitioning.

(5) We assume that the Lower Saxony Basin, and in particular the Aller-lineament plays a key role in that part of the Southern Permian Basin, as it might have acted as a barrier zone for extensional deformation triggered from the North Sea area in the north, and compressional deformation generated from the Alpine area in the south.